EXPERIMENTAL AND NUMERICAL INVESTIGATION OF THE EFFECT OF TEMPERATURE ON THE BEHAVIOUR UNDER IMPACT OF COMPOSITE SANDWICH PANELS FOR SPACE APPLICATIONS

Mathilde Jean-St-Laurent[1], Marie-Laure Dano[1] and Marie-Josée Potvin[2]

[1]Department of mechanical engineering, University Laval, Québec, Canada
Email: mathilde.jean-st-laurent.1@ulaval.ca, marie-laure.dano@gmc.ulaval.ca
[2]Canadian Space Agency, Saint-Hubert, Canada
Email: marie-josee.potvin2@canada.ca

Keywords: Composite sandwich panels, impact, quasi-static indentation, extreme temperature

Abstract
Impact and quasi-static indentation behaviours at extreme temperatures were studied for carbon-epoxy sandwich panels with Nomex honeycomb core. Different impact conditions with two sizes of hemispherical impactors were tested at room temperature, -70°C, and -150°C. Small effects of temperature are observed on the load-displacement and load-time curves, while an increase of damage has been observed at cold temperature. A numerical model to simulate the out-of-plane behaviour of the sandwich panels was developed and is also presented. The model was applied to the simulation of quasi-static indentation tests at room temperature, -70°C, and -150°C.

1. Introduction

Carbon-epoxy composite sandwich panels are considered for the fabrication of lunar exploration rovers. They offer excellent mechanical properties combined with lightness, while the core material helps with thermal insulation. On the moon, rovers will be exposed to extreme temperature variations. Indeed, temperatures can go from 120°C to -150°C [1]. In some shadowed areas, temperatures can even be lower than -200°C. Composite materials are known for their sensitivity to temperature. Temperature affects not only the mechanical properties of the material, but is also responsible for the development of internal stresses. Moreover, on the moon, the rover will work on a rugged terrain with limited ground visibility caused by the presence of lunar dust in suspension, as well as a thick layer of up to 30 cm of loose dust on the ground, leading to possible impacts with its surroundings. It is therefore essential to understand the effect of temperatures on the impact behaviour of composite sandwich panels.

Few studies have looked into the effect of temperatures on the behaviour of composite sandwich panels under impact loadings [1-4]. Amongst them, even fewer have studied impact on carbon-epoxy sandwich panels and none of them have studied temperatures as cold as -150°C. Salehi-Khojin et al. [4] have studied the effect of temperature on the impact behaviour of carbon-epoxy and hybrid carbon-kevlar-epoxy sandwich panels with a core made of honeycomb craft paper filled with polyurethane foam. They observed an increase of the size of the damaged area as temperatures decreased from 120°C to -50°C. Yang et al. [3] observed opposite results for carbon-epoxy sandwich panels with a foam core impacted at -45.6 °C, -20°C, and 82.2°C. They measured a higher residual damage depth at 120°C than -45.6°C. They associated those results with the effect of temperatures on the foam core.

Since a limited amount of literature exists on impact at extreme temperatures for sandwich panels, works on composites laminates are extremely interesting. Gómez-del Río et al. [6] have performed impact tests

at -150°C on carbon-epoxy composite laminates. They observed an increase in damage at cold temperature. Sanchez-Saez et al. [7] studied the dynamic behaviour of carbon/epoxy laminates under three point bending at extreme cold temperatures. They observed that the mechanical strength and the absorbed energy decrease with decreasing temperature from room temperature (RT) to -150°C.

Modelling of impact behaviour of composite laminates and composite sandwich panels has received a lot of attention in past decades. Indeed, experimental testing are costly and time consuming which makes the development of efficient numerical tools essential. However, most of the time, the developed model is only used at RT with only a few exceptions. Gomez del rio et al. [8] have performed impact simulations on carbon-epoxy laminates at RT, -20°C, and -150°C. The failure behaviour of the composite was based on Hou criteria [9] and included four failure modes. Yang et al. [3] developed a model to simulate impact loading at different temperatures on sandwich panels with composite skins and polymeric foam core. They used damage mechanics to model the failure of the composite.

The objective of the herein project is to study the effect of extreme cold temperatures on the low velocity impact behaviour of carbon-epoxy sandwich panels. A numerical model to simulate the out-of-plane behaviour of the panel is also developed and applied at different temperatures.

2. Material

The sandwich panel is made of woven carbon-epoxy composite skins and a Nomex honeycomb core and has the following stacking sequences: [(±45)/(0/90)/(0/90)/(±45)/core/(±45)/(0/90)/(0/90)/(±45)]. The resin is a 977-2 epoxy. The core is made of 4.76 mm hexagonal cells and has a density of 48 kg/m^3. The core is 12.7 mm thick and the total thickness of the panel is around 15.4 mm.

3. Experimentation

3.1. Experimental set-up and methodology

Impact and quasi-static indentation tests were performed. Impact tests were performed on a drop tower with a thermal chamber cooled with liquid nitrogen. The chamber was slightly modified to cool down to -150°C. During testing, specimens are clamped on a steel support with an inner diameter of 76.2 mm. An anti-rebound system is used to prevent a second impact on the specimens. An instrumented impactor is used to measure the loads.

Impact tests were all performed at 1m/s. Two hemispherical impactors were used: one with a diameter of 12.7 mm and the other with a diameter of 25.4 mm. Two masses of 5 kg and 10 kg were used with the 12.7 mm diameter impactor and three masses of 5 kg, 10 kg, and 20 kg were used with the 25.4 mm impactor. For each impact configuration, five tests were performed at RT , -70°C, and -150°C.

Quasi-static indentation tests of the sandwich panels were performed at RT, -70°C, and -150°C on a universal testing machine with a thermal chamber. Specimens were simply resting on a circular support with an inner diameter of 76.2 mm. Two hemispherical indentors were used with respectively 25.4 mm and 12.7 mm diameters. Tests were performed at a speed of 1.25 mm/min. For the 25.4 mm diameter indentor, the maximum indentation depth is 6 mm and for the 12.7 mm the maximum indentation depth is 5 mm. In both cases, complete unloading of the specimens were performed.

Prior to every test, specimens were dried in an oven to remove moisture. For the tests at cold temperatures, once the desired temperature was reached, specimens were kept at that temperature for 15 minutes before the impact or indentation test.

3.2. Results

3.2.1. Impact tests

Fig. 1 presents the load-time and load-displacement curves obtained at RT, -70°C, and -150°C for the 25.4 mm diameter impactor with the 5 kg mass. For all test cases done with the 25.4 mm diameter impactor, the behaviour is stiffer at -150°C and -70°C than it is at RT, but there is no noticeable difference between the -70°C and the -150°C test cases. For most of the test cases, loads are slightly smaller at -150°C. Finally, maximum displacements are also slightly higher at -150°C. However, the differences in the results for the three temperature cases are very limited with the 25.4 mm diameter impactor.

Fig. 2 presents the load-time curves for the 12.7 mm diameter impactor with the 5 kg and 10 kg masses. With the 12.7 mm diameter impactor, the effect of temperature is more important. The phenomenons observed for the 25.4 mm diameter impactor are more pronounced with the 12.7 mm diameter impactor. In the case of the tests done with the 10 kg mass at -70°C and -150°C, the impactor hits the bottom skin. This is visible on the load versus time curves, which show a second bell (Figure 2 b). Moreover, the smooth curve for the second impact at -70°C indicates a limited amount of damage on the bottom skin, while at -150°C, the load drops in the second part of the curves indicate the development of damage on the bottom skin.

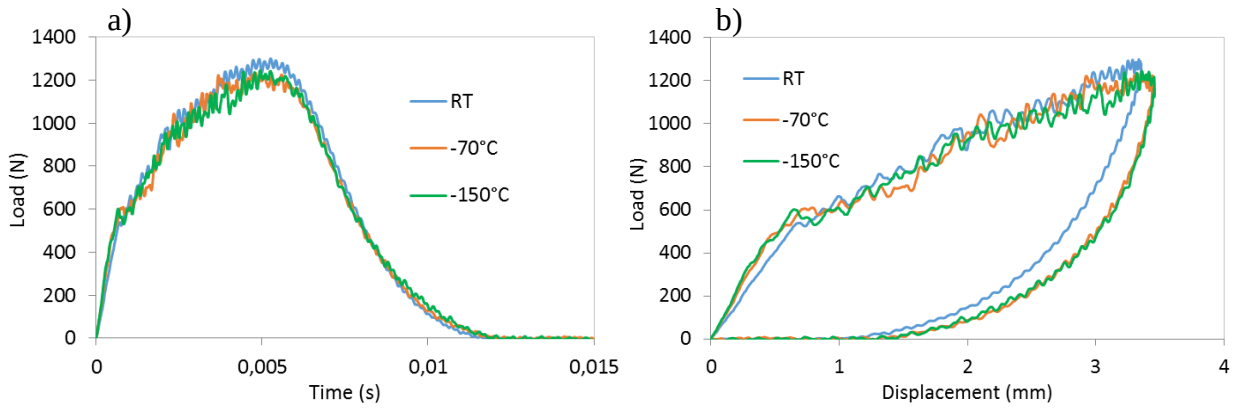

Figure 1. a) Load-time and b) load-displacement curves for the 5 kg mass with the 25.4 mm diameter impactor at RT, -70°C, and -150°C.

3.2.2. Quasi-static indentation tests

Fig.3 presents the typical load-displacement curves obtained for the quasi-static indentation tests for both indentors at all three temperatures. The curves show that the load reaches higher values at RT than at -70°C and -150°C for both sizes of indentors. Moreover, upon unloading, the load reaches a value of zero at a larger indentor displacement for the -150°C curve. It indicates a larger residual depth of indentation at -150°C. For the 12.7 mm indentor at -150°C (Fig. 3 b), the load starts to decrease significantly before the displacement reaches 5 mm. This was observed for two specimens out of three.

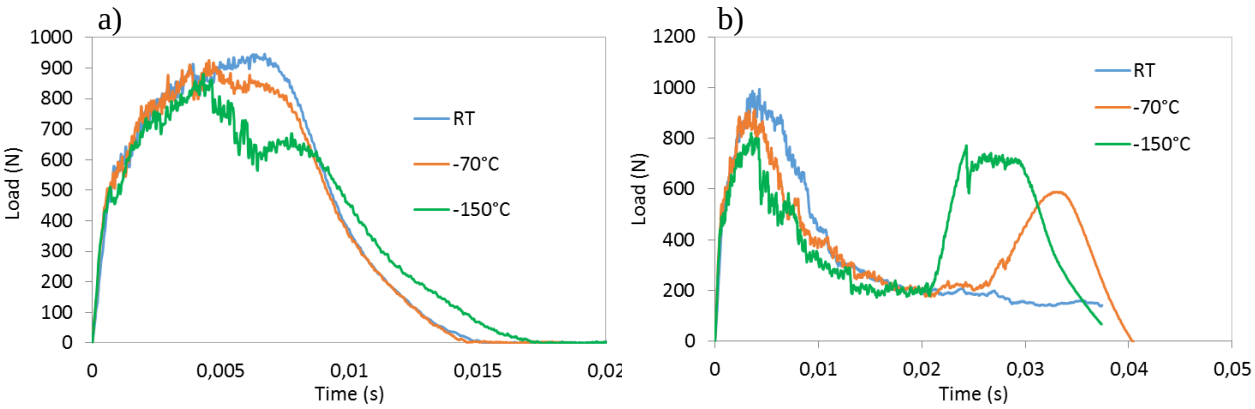

Figure 2. Load-time curves for a) the 5 kg mass and b) the 10 kg mass with the 12.7 mm diameter impactor at RT, -70°C, and -150°C.

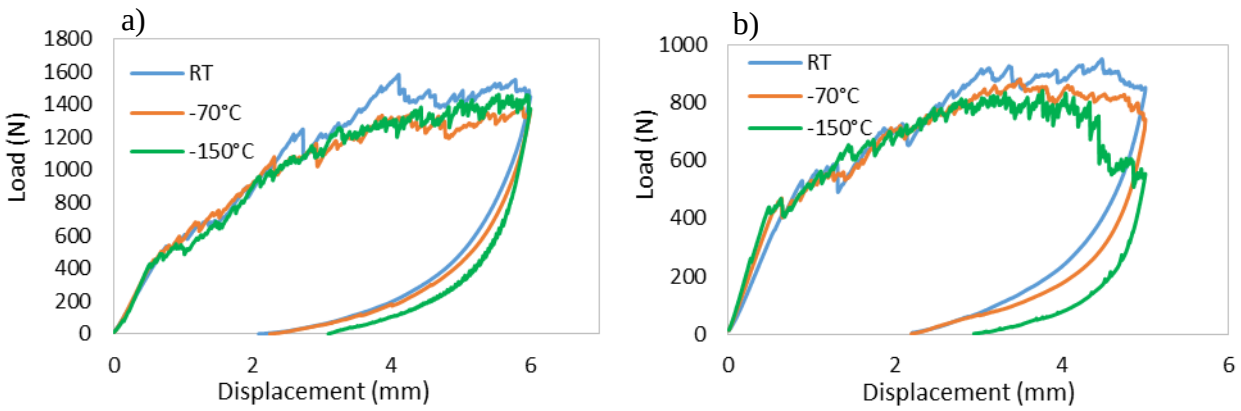

Figure 3. Load-displacement curves for a) the 25.4 mm diameter indentor and b) the 12.7 mm diameter indentor at RT, -70°C, and -150°C.

3.3. Damage analysis

Visual inspections of all the impacted specimens were performed. For most impact conditions, a larger number of cracks are generally observed on the upper skin with decreasing temperature. The depth of the damage area is also larger at -150°C. In the case of the 25.4 mm diameter impactor with the 5 kg mass, damage is barely visible at all three temperatures. For the 12.7 mm impactor with the 10 kg mass, there are visible damages on the bottom skin for the specimens impacted at -150°C.

4. Simulation

4.1. General description

Numerical simulations of the quasi-satic indentation with the 25.4 mm impactor were performed at RT, -70°C, and -150°C. The numerical simulations were performed using ABAQUS/Explicit. Each ply of the composite skin is modeled as a different part with one element through its thickness. C3D8R elements are used. The same elements are used for the core. Contact is applied between the indentor and

the specimen surface. The sandwich panel model is circular with a 76.2 m diameter. The nodes on the edge of the last ply of the bottom skin are fully constraint in displacement.

4.2. Composite material model

4.2.1. Model description

The in-plane behaviour of the composite material is linear elastic orthotropic and includes damage mechanics at the mesoscale level [10,11]. Plies are homogenous and damage is considered constant through the thickness of the plies. Three damage variables are used: d_1 and d_2 in the warp and weft directions respectivly and d_{12} associated with in-plane shear behaviour. The in-plane compliance matrix is given by :

$$S = \begin{bmatrix} \frac{1}{E_1(1-d_1)} & \frac{-\upsilon_{12}}{E_1} & 0 \\ \frac{-\upsilon_{12}}{E_1} & \frac{1}{E_2(1-d_2)} & 0 \\ 0 & 0 & \frac{1}{2G_{12}(1-d_{12})} \end{bmatrix} \quad (1)$$

In the warp and weft directions, the onset of damage is associated with a strain at failure. Then, the damage variables evolved linearly with the strain up to a maximum strain. The maximum strain is determined with the fracture energy (G_c) and the ultimate strength (X_{ii}) and is also dependant of a characteristic length of the element (l_c). The use of the fracture energy is based on Bažant and Oh band criteria [12] and is used in many damage models [13]. The expression for the maximum strain is given by:

$$\varepsilon_{ii,max} = \frac{2G_c}{X_{ii} l_c}, \quad (ii = 11, 22) \quad (2)$$

The shear behaviour is based on the work of Hochard et al. [11]. The combination of a damage variable and a plastic hardening model is used to model the non-linear in-plane shear behaviour. The damage evolution is function of thermodynamic forces :

$$y_{ii} = \frac{{\sigma_{ii}}^2}{2E_i(1-d_i)^2}, \quad (ii = 11, 22)$$
$$y_{12} = \frac{{\sigma_{12}}^2}{2G_{12}(1-d_{12})^2} \quad (3)$$

An equivalent force is used to take into account the effect of tensile stress in the warp and weft directions on the in-plane shear damage. Indeed, tensile stresses in the warp and weft directions induce microcracks. Those cracks will contribute to shear damage evolution. The equation for the equivalent force is given by:

$$Y_{eq} = \alpha\langle Y_{11}\rangle_+ + \alpha\langle Y_{22}\rangle_+ + Y_{12} \quad (4)$$

where α is a coupling parameter. The evolution of the damage variable d_{12} is given by:

$$d_{12} = \frac{\sqrt{Y_{eq}} - \sqrt{Y_0}}{\sqrt{Y_C} - \sqrt{Y_0}} \tag{5}$$

where Y_{eq} et Y_c are paremeters of the damage variable d_{12} evolution law. The elastic field is function of the effective shear stress:

$$f = \sqrt{\left(\frac{\sigma_{12}}{(1-d_{12})}\right)^2} - R_0 - R(p) \tag{6}$$

where R_0 is the initial shear stress threshold value for the inelastic strain and $R(p)$ is the hardening law defined by:

$$R(p) = Cp^k \tag{7}$$

where C and k are parameters of the hardening law, while p is the cumulated plastic strain.

Delamination is taken into account with a quadratic criteria [14] and simple degradation rules for the out-of-plane properties. The stress in the out-of-plane direction (σ_{33}) is only considered if it is in tension for the calculation of the criteria. The criteria is given by :

$$\left(\frac{\langle\sigma_{33}\rangle_+}{X_{33}}\right)^2 + \left(\frac{\sigma_{13}}{X_{13}}\right)^2 + \left(\frac{\sigma_{23}}{X_{23}}\right)^2 = 1 \tag{8}$$

where X_{33}, X_{13} et X_{23} represent respectively the out-of-plane tensile strength and out-of-plane shear strengths.

4.2.2. Model parameter identification

The in-plane elastic and failure properties in tension were obtained at RT, -70°C, and -130°C from experimental investigations [15]. The properties obtained at -130°C are used for the simulations at -150°C. The elastic and non-linear shear properties were also obtained from experimental investigations at RT, -70°C, and -150°C. Cyclic shear tests were indeed performed at those three temperatures. The value of fracture energy used in the evolution laws of d_{11} and d_{22} is estimated for the moment and will be validated experimentally. For the present simulations, its value is kept constant at all temperatures. The out-of-plane elastic and failure properties used for the delamination model were estimated from literature [16,17].

4.3. Nomex honeycomb model

The Nomex honeycomb core model is homogenized. The behaviour is elastic orthotropic with an isotropic plastic model. The yield stress used for the simulation is the initial plateau stress obtained experimentally. The out-of-plane compression modulus was obtained experimentally. The other elastic properties were obtained from technical data sheets from the manufacturer or estimated [18]. As for the properties at cold temperatures, out-of-plane compression tests were performed at -70°C and -150°C as well. The out-of-plane elastic modulus increased with temperature decreasing. The stresses of the plateau were slightly inferior at -70°C and -150°C.

4.4. Results

Fig. 4. presents the load-displacement curve obtained from simulations at RT, -70°C, and -150°C and the experimental curve at RT. The simulations were only performed up to an indentation of 3 mm. Passed this point, the model will have to be improved in order to reproduce properly the important level of damage seen by the specimens. The model developed predicts well the fisrt part of the indentation tests. The load associated with the first damages occurring in the skin is well predicted. The effect of temperature on the load-displacement curves seems also in agreement with the experimental results (Fig. 3 a).

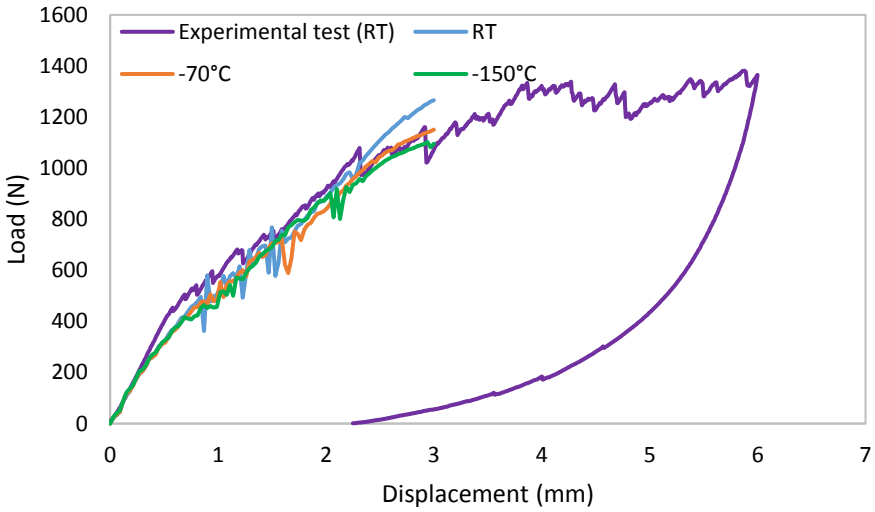

Figure 4. Load-displacement curves for the simulation at RT, -70°C, and -150°C.

5. Conclusions

Impact tests at extreme cold temperatures were performed. The results showed that damage increases with temperature decreasing and that the behaviour of the sandwich panels impacted with the smallest impactor was more affected by cold temperatures.

Numerical simulations of the quasi-static indentation tests were performed. Results are in good agreement with the experimentation altougth the whole tests have not been reproduced. The model will have to be improved in order to reproduce larger extent of damage. This model will then be used to perform numerical simulations of the impact tests at different temperatures as well.

Acknowledgments

The authors fully acknowledge the supports from the National Sciences and Engineering Research Council of Canada and the Canadian Space Agency.

References

[1] J. J. Zakrajsek, D. P. Mckissock, J. M. Woytach, J. F. Zakrajsek, F. B. Oswald, K. J. Mcentire, G. M. Hill, P. Abel, D. J. Eichenberg, and T. W. Goodnigth. Exploration rover concepts and development challenges. *Proceedings of the First AIAA Space Exploration Conference, Orlando, USA*, January 30-February 1 2005.

[2] M. D. Erickson, A. R. Kallmeyer, and K. G. Kellogg. Effect of temperature on the low-velocity impact behavior of composite sandwich panels. *Journal of Sandwich Structures and Materials*, 7(3):245–264, 2005.

[3] P. Yang, S. S. Shams, A. Slay, B. Brokate, and R. Elhajjar. Evaluation of temperature effects on low velocity impact damage in composite sandwich panels with polymeric foam cores. *Composite Structures*, 129:213–223, 2015.

[4] A. Salehi-Khojin, M. Mahinfalah, R. Bashirzadeh, and B. Freeman. Temperature effects on Kevlar/hybrid and carbon fiber composite sandwiches under impact loading. *Composite Structures*, 78(2):197–206, 2007.

[5] A. Sakly, A. Laksimi, H. Kebir, and S. Benmedakhen. Experimental and modelling study of low velocity impacts on composite sandwich structures for railway applications. *Engineering Failure Analysis*, 68:22–31, 2016.

[6] T. Gómez-del Río, R. Zaera, E. Barbero, and C. Navarro. Damage in CFRPs due to low velocity impact at low temperature. *Composites Part B: Engineering*, 36(1):41–50, 2005.

[7] S. Sánchez-Sáez, E. Barbero, and C. Navarro. Analysis of the dynamic flexural behaviour of composite beams at low temperature. *Composites Science and Technology*, 67(11-12):2616–2632, 2006.

[8] T. Gómez-del-Rio, R. Zaera, and C. Navarro. Prediction of the effect of temperature on impact damage in carbon / epoxy laminates. *Journal de Physique IV France*, 110:699–704, 2003.

[9] J. P. Hou, N. Petrinic, C. Ruiz, and S. R. Hallett. Prediction of impact damage in composite plates. *Composites Science and Technology*, 60(2):273–281, 2000.

[10] P. Ladevèze. A damage computational approach for composites: Basic aspects and micromechanical relations. *Computational Mechanics*, 17(1-2):142–150, 1995.

[11] C. Hochard, P. A. Aubourg, and J. P. Charles. Modelling of the mechanical behaviour of woven-fabric CFRP laminates up to failure. *Composites Science and Technology*, 61(2):221–230, 2001.

[12] Z. P. Bažant and B. H. Oh. Crack band theory for fracture of concrete. *Materials and Structures*, 16(3):155–177, 1983.

[13] I. Lapczyk and J. A. Hurtado. Progressive damage modeling in fiber-reinforced materials. *Composites Part A : applied science manufacturing*, 38(11):2333–2341, 2007.

[14] J. Brewer and P. Lagace. Quadratic stress criterion for initiation of delamination. *Journal of Composite Materials*, 22(12):1141–1155, 1988.

[15] M. Jean-St-Laurent, M-L. Dano, and M-J. Potvin. In-plane mechanical behaviour of composite laminates and out-of-plane behaviour of composite sandwich panel under extreme temperatures. *Proceedings of the Canadian International Conference on Composite Materials CANCOM2017, Ottawa, Canada*, July 17-20, 2017.

[16] A. Turon, C. G. Dávila, P. P. Camanho, and J. Costa. An engineering solution for mesh size effects in the simulation of delamination using cohesive zone models. *Engineering Fracture Mechanics*, 74(10):1665–1682, 2007.

[17] *Composite Materials Handbook Volume2. Polymer matrix composites: Materials properties.* SAE International, 2012.

[18] S. Heimbs, S. Schmeer, P. Middendorf, and M. Maier. Strain rate effects in phenolic composites and phenolic-impregnated honeycomb structures. *Composites Science and Technology*, 67(13):2827–2837, 2007.